Two-Dimensional Phase Unwrapping for the Design of Distributed Phase Plates

Melisa Gao

Laboratory for Laser Energetics, University of Rochester
Rochester, New York 14623-1299

1. ABSTRACT

When the surface of a distributed phase plate (DPP) is designed via the phase retrieval method, the resulting phase profile is discontinuous because of the use of the inverse tangent function. The precise manufacturing of a discontinuous phase plate is impossible, however, and any imperfections scatter the laser beam out of the desired far-field intensity pattern. Phase unwrapping is therefore employed to create a continuous phase plate by removing discontinuities between adjacent data points.

An unwrapping algorithm that attempts to smooth over the data while retaining the desired far-field mapping was successfully implemented and will be integrated into the phase retrieval method for future calculations of DPPs. The weighted form of the algorithm is expected to increase its effectiveness at unwrapping uncertain data.

2. INTRODUCTION

A diffraction-limited focal spot is governed by the focal length (f), wavelength (λ), and diameter of the laser beam (D). On the University of Rochester Laboratory for Laser Energetics OMEGA laser system, this yields a focal spot approximately 2 μm in diameter,

$$\frac{f\lambda}{D} = \frac{1.8m(351nm)}{28cm} = 2\mu m, \tag{1}$$

as opposed to the 1-mm target size. This desired focal spot size could be achieved by simply defocusing the laser (i.e. placing the target in front of the focal plane of the lens), but the intensity profile would not be flat enough and is uncontrollable.

To avoid these problems, a distributed phase plate (DPP) is used. A DPP is a plate of glass with an uneven surface profile that adds phase to the rays in the near field, thereby manipulating the far-field image (Fig. 1). These phase changes effectively spread the energy out across the entire target in the far field and define a well-controlled average intensity pattern.

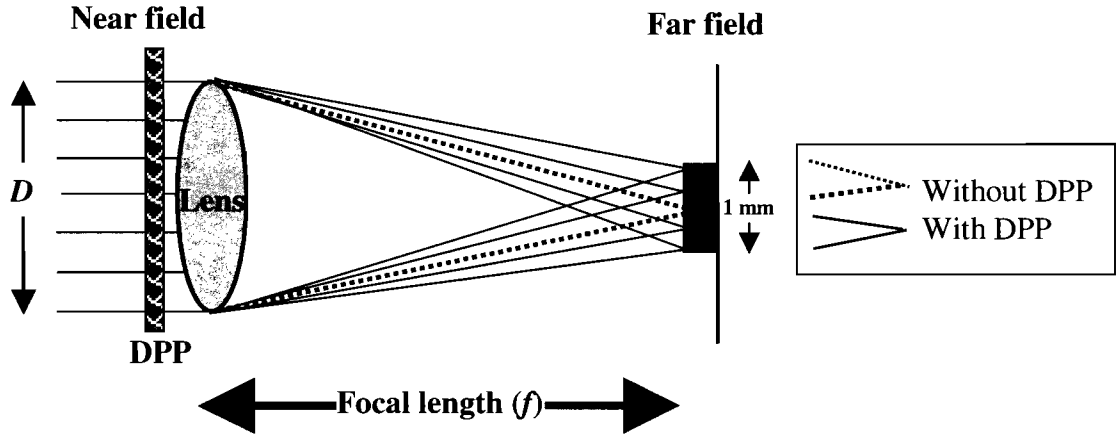

Fig. 1. A DPP spreads the beam across the 1-mm target by adding phase to the incident rays.

The far-field intensity pattern generated by a DPP is actually composed of a finely-grained structure called a speckle, with an average diameter given by Eq. (1). This speckle pattern is smoothed out in a time-integrated sense using smoothing by spectral dispersion (SSD), which randomly changes the speckle pattern on a small time-scale.

A distributed phase plate can be designed to produce almost any desired far-field average intensity pattern. The calculation of a DPP is based on the concept that the complex-valued near and far fields are related through Fourier transforms[1] (Fig. 2). The Fourier transform of the near field, which is a function of the phase and amplitude (defined as the square root of the intensity) of the laser beam as it enters the lens, is proportional to the phase and amplitude of the far field. The inverse Fourier transform of the far field is the near field. Fourier transforms are a one-to-one process, so if the near field is known, the far field can be uniquely determined, and vice versa.

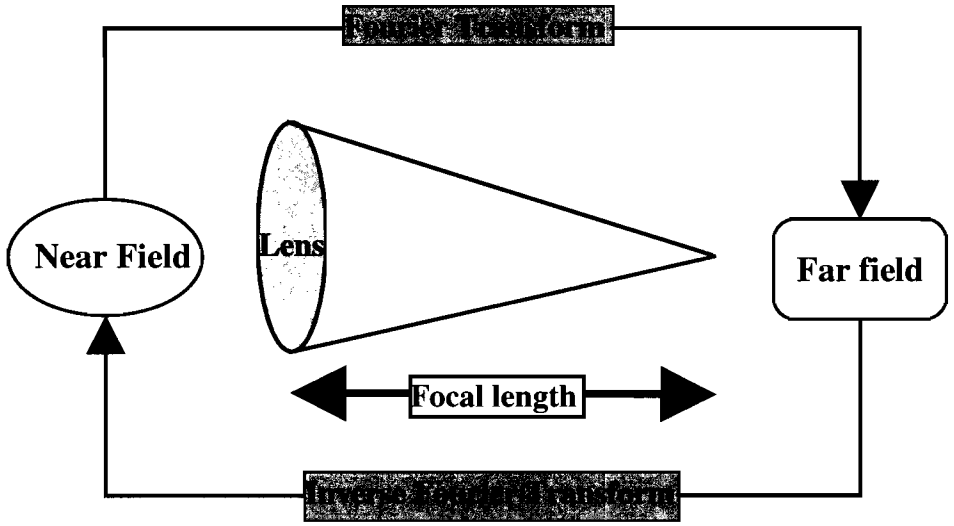

Fig. 2. The far field is the Fourier transform of the near field, which is the inverse Fourier transform of the far field.

3. THE PHASE RETRIEVAL METHOD

The phase retrieval method (Fig. 3) designs the surface of a DPP that will generate a desired far-field intensity pattern[2]. Initially, the intensity pattern of the near field, I_{NF}, is given (as a property of the laser beam itself), and the desired far-field intensity pattern I_{FF} is chosen. For the first step of the phase retrieval method, the phase profile of the near field is initialized to a guess, P_0. The Fourier transform of this initial near field (I_{NF} and P_0) is the far field, where the calculated far-field intensity pattern is replaced by I_{FF}. The inverse Fourier transform of the new far field (the calculated phase profile P_1 and known intensity pattern I_{FF}) is the calculated near field for the next iteration of the sequence.

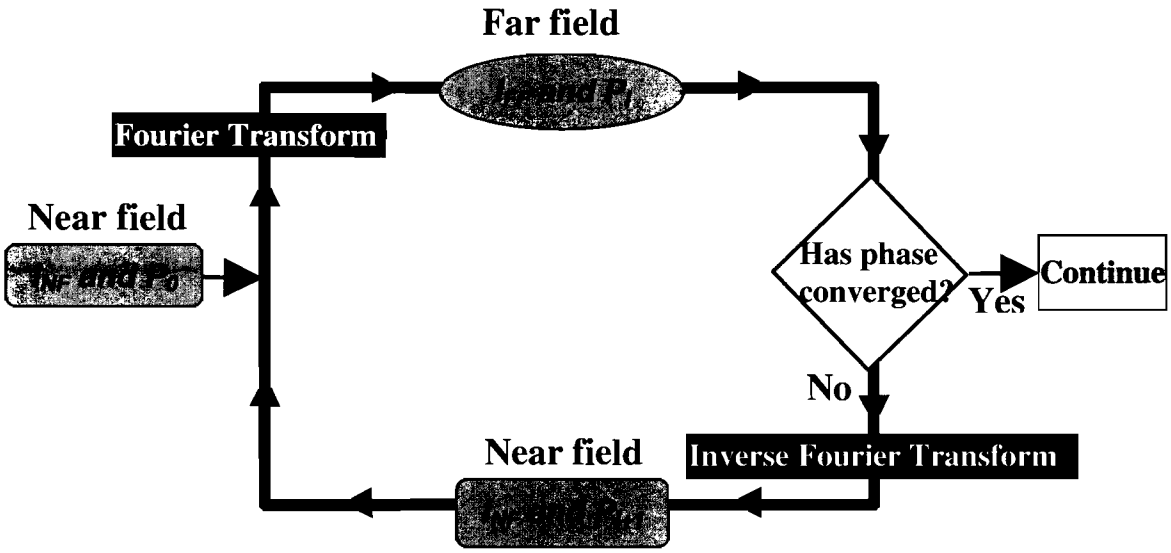

Fig. 3. The phase retrieval method is an iterative sequence used to design a DPP that will calculate a desired far-field intensity pattern.

In the near field, the calculated phase P_2 is retained while the resultant intensity is discarded and replaced with the known I_{NF}. This new near field (P_2 and I_{NF}) is Fourier-transformed to calculate the new far field, and the process repeats.

Each time, the calculated phase profile P_i is retained while the calculated intensity

pattern is replaced by I_{NF} or I_{FF}. After multiple iterations, the intensity and phase profiles in the near and far field eventually converge upon a solution ($P_i \cong P_{i+1}$). At this point, a near-field phase profile has been calculated that, with the specific laser beam intensity, will generate the desired far-field intensity pattern. Since a DPP serves to add phase to a uniform beam, the appropriate DPP is simply this calculated near-field phase profile.

A problem arises, however, in the actual implementation of the calculated DPP phase profile. Note that the inverse tangent function is needed to calculate the phase from the complex value obtained from the Fourier transform. Sharp 2π discontinuities in the calculated phase arise, since a single branch of the inverse tangent function is restricted to the interval of $[-\pi, \pi)$. Because of manufacturing limitations, attempting to create this discontinuous DPP will result in inaccuracies in the plate. These imperfections lead to the scatter of light in the far field, which decreases the efficiency of the distributed phase plate.

Thus after the phases converge to signal the conclusion of the phase retrieval method, the calculated phase profile is unwrapped (Fig. 4) via the cosine transform

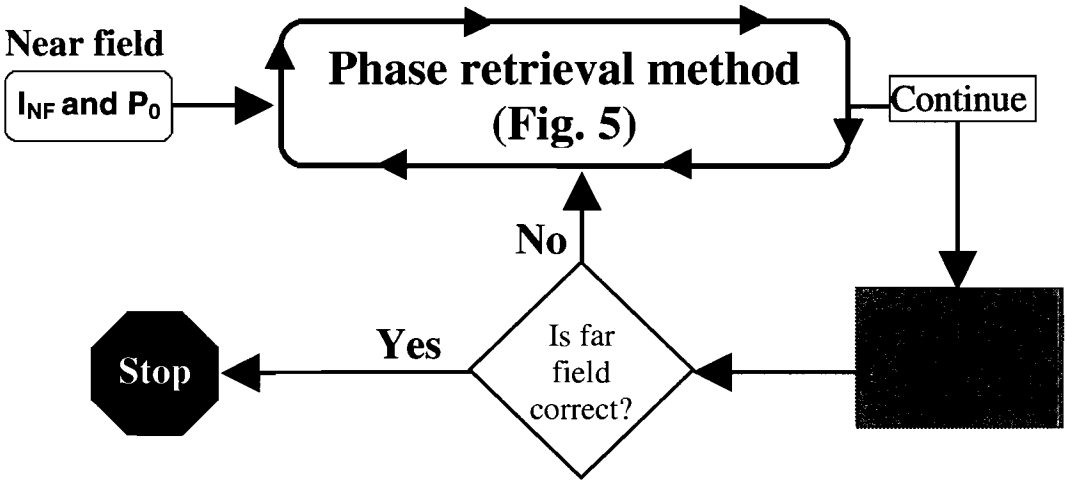

Fig. 4. Multiple iterations of the phase retrieval method and unwrapping process are performed as needed to generate the desired far-field intensity pattern.

technique to remove discontinuities. Phase data has ambiguities of 2π, so phase unwrapping is employed to construct a smooth function that attempts to retain the phase data of a wrapped function with discontinuities of 2π. That is, the values of the unwrapped function are ideally equal to the values of the wrapped function plus integral multiples of 2π, so the far-field image remains unaffected.

Because the unwrapping algorithm must smooth over noise in the data, however, it can cause loss of data that changes the far field image. The unwrapped phase profile is therefore checked for accuracy (i.e. whether it produces the desired far field). If necessary, the method is repeated until a smooth, unwrapped distributed phase plate has been calculated.

4. UNWRAPPING

Unwrapping is the reconstruction of a smooth function given its values on the interval of $[-\pi, \pi)$. The wrapped version of a continuous one-dimensional function is easily unwrapped by detecting discontinuities and adding or subtracting 2π over selected intervals as necessary. In Fig. 5a, for example, the discontinuity at $x = 0.25$ can be eliminated by shifting up by 2π the section of the function to the right of it. By examining all the discontinuities in the function in this fashion, a smooth curve is reconstructed. Note that this unwrapped result is not unique; the entire function can be shifted by any constant phase factor.

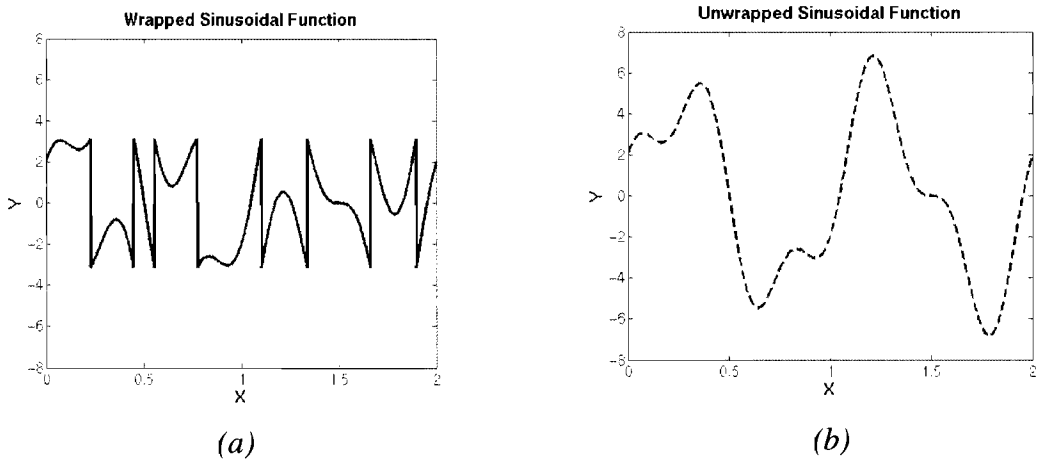

(a) *(b)*

Fig. 5. A smooth, one-dimensional function of the sum of sines and cosines is reconstructed by shifting discontinuous regions in the wrapped function by multiples of 2π.

Unwrapping a two-dimensional function is not as straightforward, however, as shifting values by $\pm 2\pi$ in one dimension might result in discontinuities in the other direction. A single pixel of noise would become a spike in the unwrapped function, and since this happens independently in each direction, it may be impossible to generate a smooth function.

5. THE COSINE TRANSFORM TECHNIQUE FOR PHASE UNWRAPPING

The cosine transform technique is a method of finding a least-squares solution for the unwrapped function[3]. Let ϕ and ψ be the unwrapped and wrapped functions, respectively, both on an M by N grid. Note that the wrapped and unwrapped functions have similar derivatives, where derivatives are estimated as the difference between neighboring points. These values will henceforth be referred to as the *finite difference* at a point. In addition to providing a straightforward method of approximating a derivative, this allows us to quantify the derivative at every point, including discontinuities.

In continuous regions in the wrapped function, the finite differences of the wrapped and unwrapped functions are equal. At discontinuities of 2π in the wrapped function, the finite differences are unequal but differ only by $\pm 2\pi$. Note that while all finite differences in the (continuous) unwrapped function will be relatively small, those at discontinuities of the wrapped function will be much larger values.

For example, suppose we have the adjacent data values 3.140 and 3.240 on the unwrapped function, with an estimated difference of $3.240 - 3.140 = 0.100$. On the wrapped function, the first data point is unchanged while the second becomes $3.240 - 2\pi = -3.043$. The estimated difference for the wrapped function is therefore $-3.043 - 3.140 = -6.183$. Thus the two estimated differences are off, but only by an integral number of 2π. Specifically, if we define the function *Wrap* to return a value on the interval $[-\pi, \pi)$ by adding integral multiples of 2π, then 0.100 = *Wrap* (-6.183). Moreover, the *Wrap* relationship holds true throughout continuous regions as well, since finite differences are equal (as established above).

Generalizing this concept, we see that for an ideal solution for ϕ,

$$\begin{aligned}\phi_{i+1,j}-\phi_{i,j} &= Wrap(\psi_{i+1,j}-\psi_{i,j}) \\ \phi_{i,j+1}-\phi_{i,j} &= Wrap(\psi_{i,j+1}-\psi_{i,j}),\end{aligned} \tag{2}$$

where $0 \le i \le M-1$ and $0 \le j \le N-1$. That is, the finite differences of the wrapped function equal the wrapped version of the finite differences of the unwrapped function.

By extension, the best solution for ϕ is that which satisfies Eq. (2) by minimizing the sum

$$\sum_{i=0}^{M-2}\sum_{j=0}^{N-1}\left[(\phi_{i+1,j}-\phi_{i,j})-Wrap(\psi_{i+1,j}-\psi_{i,j})\right]^2+\sum_{i=0}^{M-1}\sum_{j=0}^{N-2}\left[(\phi_{i,j+1}-\phi_{i,j})-Wrap(\psi_{i,j+1}-\psi_{i,j})\right]^2 \tag{3}$$

.

This least-squares solution allows for smoothing over of noise pixels to create the best overall fit.

According to Hunt's matrix formulation[4], Eq. (3) can be simplified to

$$\phi_{i+1,j}+\phi_{i-1,j}+\phi_{i,j+1}+\phi_{i,j-1}-4\phi_{i,j}=\rho_{i,j}, \tag{4}$$

where

$$\rho_{i,j}=Wrap(\psi_{i+1,j}-\psi_{i,j})-Wrap(\psi_{i,j}-\psi_{i-1,j})+Wrap(\psi_{i,j+1}-\psi_{i,j})-Wrap(\psi_{i,j}-\psi_{i,j-1}).$$

Through simple algebraic manipulation, Eq. (4) becomes

$$\begin{aligned}\rho_{i,j} &= \left[(\phi_{i+1,j}-\phi_{i,j})-(\phi_{i,j}-\phi_{i-1,j})\right]+\left[(\phi_{i,j+1}-\phi_{i,j})-(\phi_{i,j}-\phi_{i,j-1})\right] \\ &= (\phi_{i-1,j}-2\phi_{i,j}+\phi_{i+1,j})+(\phi_{i,j-1}-2\phi_{i,j}+\phi_{i,j+1}),\end{aligned} \tag{5}$$

which is the discrete version of Poisson's equation,

$$\rho(x,y)=\frac{\partial^2}{\partial x^2}\phi(x,y)+\frac{\partial^2}{\partial y^2}\phi(x,y). \tag{6}$$

We now use the form of the forward and inverse discrete cosine transform[5] (DCT) below to solve Eq. (5) for $\phi_{i,j}$:

$$Forward: C_{i,j} = \sum_{i=0}^{M-1}\sum_{j=0}^{N-1} 4x_{i,j} \cos\left[\frac{\pi}{2M} m(2i+1)\right] \cos\left[\frac{\pi}{2N} n(2j+1)\right]$$
$$Inverse: x_{i,j} = \frac{1}{MN} \sum_{i=0}^{M-1}\sum_{j=0}^{N-1} w_1(m) w_2(n) C_{i,j} \cos\left[\frac{\pi}{2M} m(2i+1)\right] \cos\left[\frac{\pi}{2N} n(2j+1)\right], \quad (7)$$

where $w_1(m) = ½$, m = 0,
$w_1(m) = 1$, $1 \le m \le M-1$
$w_2(m) = ½$, n = 0,
$w_2(m) = 1$, $1 \le n \le N-1$.

The discrete cosine transforms of $\phi_{i,j}$ and $\rho_{i,j}$ ($\hat{\phi}_{i,j}$ and $\hat{\rho}_{m,n}$, respectively) according to the form in Eq. (7) are substituted into Eq. (5). Solving for $\hat{\phi}_{i,j}$ in terms of the known values $\hat{\rho}_{m,n}$, we obtain

$$\hat{\phi}_{i,j} = \frac{\hat{\rho}_{m,n}}{2\left[\cos\left(\frac{\pi m}{M}\right) + \cos\left(\frac{\pi n}{N}\right) - 2\right]}. \quad (8)$$

The inverse DCT of $\hat{\phi}_{i,j}$ yields the unwrapped phase $\phi_{i,j}$.

Thus the cosine transform technique for phase unwrapping involves three steps: finding the values of $\hat{\rho}_{m,n}$ by performing the forward DCT on the known array $\rho_{i,j}$, substituting into Eq. (5) to find $\hat{\phi}_{i,j}$, and taking the inverse DCT of $\hat{\phi}_{i,j}$ to calculate the values of $\phi_{i,j}$.

6. RESULTS

To test the algorithm's effectiveness, the wrapped version of a smooth DPP was unwrapped using the cosine transform technique (Fig. 6). In the reconstructed phase profile, discontinuities of 2π were successfully removed and noise spikes eliminated, resulting in a smooth function that retains the phase data of the original DPP.

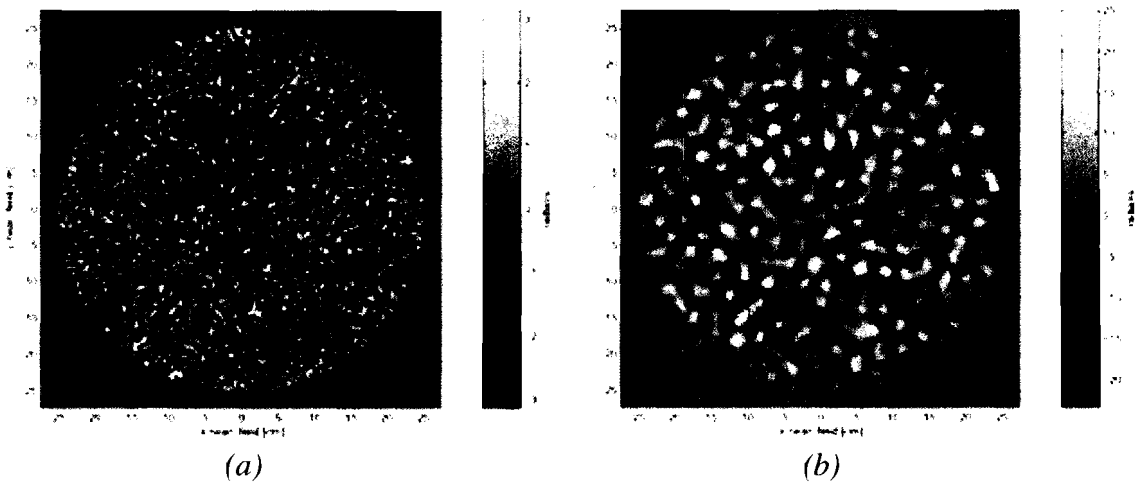

(a) *(b)*

Fig. 6. The phase profile of a wrapped DPP *(a)* is unwrapped to recover the phase of a smooth DPP *(b)* using the cosine transform technique.

This algorithm fails to account for uncertainty in data, however, such as at the border of the DPP. It tries to eliminate the discontinuity between the edge of the DPP and the area of no data. Though this does not present a problem in this particular phase plate, as the errors occur only beyond the data boundary of the DPP, it may affect the plate in other instances. Implementing the weighted Picard algorithm[6] that factors in assigned confidence levels is expected to minimize this problem. Assigning a confidence of zero to areas of no data, for example, would prevent the rest of the data from being corrupted as the algorithm tries to reconcile the discontinuities.

7. CONCLUSION

The cosine transform technique was successful in returning a distributed phase plate with a continuous surface profile that generates the desired far-field intensity pattern on target. The algorithm will be integrated into the phase retrieval method for future calculations of DPPs. The smooth DPP surface profiles generated will be more efficient, with minimal scatter of light.

Any problems encountered with uncertainty in data or noise pixels are expected to be corrected by assigning a weight to each data point via the Picard method. This will result in an even more effective DPP, thereby improving the accuracy of the far field intensity mapping as compared to the desired pattern.

8. ACKNOWLEDGEMENTS

Special thanks first and foremost to my advisor, Dr. John A. Marozas, whose guidance throughout the summer and beyond was indispensable and without whom none of this would have been possible. I am grateful to Dr. R. S. Craxton, who invited me to be a part of this experience, and the other summer high school students, who were always there to provide either a fresh perspective on my research project or a much-needed break from it. Finally, to Dr. R. Epstein and the many others at LLE whom I was fortunate enough to get to know: your approachability and companionship made this opportunity an unforgettable one. Thank you.

9. REFERENCES

1. R. N. Bracewell, *The Fourier Transform and Its Applications*, 2nd ed., rev., McGraw-Hill Series in Electrical Engineering. Circuits and Systems (McGraw-Hill, New York, 1986).

2. J. R. Fienup, "Phase retrieval algorithms: a comparison," Appl. Opt. **21** (15), 2758-2769 (1982).

3. D. C. Ghiglia and L. A. Romero, "Robust two-dimensional weighted and unweighted phase unwrapping that uses fast transforms and iterative methods," J. Opt. Soc. Am. A **11**, 107-17 (1994).

4. B. R. Hunt, "Matrix formulation of the reconstruction of phase values from phase differences," J. Opt. Soc. Am. **69**, 393-99 (1979).

5. W. H. Press, B. P. Flannery, S. A. Teukolsky, and W. T. Vetterling, *Numerical Recipes: The Art of Scientific Computing* (Cambridge U. Press, Cambridge, 1986).

6. D. C. Ghiglia and M. D. Pritt, *Two-dimensional phase unwrapping: theory, algorithms, and software* (John Wiley and Sons, New York, 1998).